Post-glacial readjustment, sea-level variations, subsidence and erosion along Italian coasts

P. Stocchi[1], L. Girometti[2], G. Spada[2], M. Anzidei[3] and F. Colleoni[4]

[1] *DEOS, Faculty of Aerospace Engineering, Delft University of Technology, The Netherlands*
[2] *Istituto di Fisica, Università "Carlo Bo", Urbino, Italy*
[3] *Istituto Nazionale di Geofisica e Vulcanologia, Roma, Italy*
[4] *Laboratoire de Glaciologie et Géophysique de l'Environnement, Grenoble, France*

(Received: March 31, 2008; accepted: July 4, 2008)

ABSTRACT Ongoing sea-level variations and vertical land movements, measured by tide gauges as well as by continuous GPS stations in Italy, stem from several factors acting on different spatiotemporal scales. Contrary to tectonic and anthropogenic effects, characterized by a heterogeneous signal, the melting of the late-Pleistocene ice sheets results in a smooth long-wavelength pattern of sea-level variation and vertical deformation across the Mediterranean, mostly driven by the melt water load. In this work, we define upper and lower bounds of the effects of glacial isostatic adjustment (GIA) on current sea-level variations and vertical movements along the coasts of Italy. For various mantle viscosity profiles, we explore to what extent the spatial variability of the observed rates may be attributed to a delayed isostatic recovery of both solid Earth and geoid. We find that long-wavelength patterns of sea level change are tuned by GIA, and that the coastal retreat in Italy is broadly correlated with the expected present-day rates of sea-level variations.

1. Introduction

The sea level is the offset between the surface of the geoid and that of the solid Earth at a given time (Farrell and Clark, 1976). The melting of ice sheets and glaciers causes a global (but not uniform) redistribution of the ocean mass, thus leading to a new sea level. The offset between the new and the old sea level is referred to as sea level change, which can be described by the sum of three terms. The first (eustatic term) is the globally uniform variation that we would observe for a rigid, non gravitating Earth. The second and the third are due to geoid height variations and ground vertical deformations associated to ice and water loads, respectively. These latter terms have a complex spatiotemporal variability, being also dependent upon the delayed viscoelastic response of the solid Earth [see e. g. Farrell and Clark (1976) and Spada and Stocchi (2006) for a review]. The melting of Pleistocene ice sheets has resulted in a widespread variable sea level change that defines several zones where the geoid has been affected in similar ways, showing sea level curves of equal shape (Farrell and Clark, 1976; Clark and Lingle, 1979). In the Mediterranean, these zones have been recently studied by Stocchi and Spada (2007).

Middle-to-late Holocene geological indicators along the Italian coastlines and coastal archaeological remains of the Roman period (~2500 BP) show that, since the end of the deglaciation, the sea level rose to, and never exceeded, the present- day datum (Pirazzoli, 1991,

2005; Lambeck *et al.*, 2004a). The general shape of the relative Holocene relative sea-level curves, expected in Italy is peculiar of enclosed basins, where melt-water loading deforms the sea floor thus producing a widespread subsidence (Lambeck and Purcell, 2005; Stocchi and Spada, 2007). The northern and central coasts of Italy are potentially the most affected by the process of isostatic adjustment of the former Alpine and Fennoscandian ice sheets (Stocchi *et al.*, 2005), since ice unloading and the related forebulge collapse shape the overall pattern of land subsidence to a distance of a few thousands kilometres from the ice centers (Lambeck and Johnston, 1995).

Our aim is to compare model predictions with observations at sites where tide gauges and continuous GPS time-series are available and to establish trade offs between various factors currently contributing to sea-level change and subsidence (or uplift) in Italy. Assuming as valid the ICE5G chronology for the former late-Pleistocene ice sheets (Peltier, 2004) and various plausible mantle viscosity profiles, we solve the "Sea Level Equation" (Farrell and Clark, 1976) to estimate current rates of sea-level variations induced by glacial isostatic adjustment (GIA) and vertical deformations in Italy and to discuss their relationship with instrumental observations. In the last part of the paper, we reveal a long-wavelength correlation between the pattern of coastal retreats along the Italian coasts and the current GIA-induced sea-level variations.

2. Methods

In this paper, GIA-induced sea level change (S), vertical displacement (U), and geoid height variation (N) are computed by means of the public-domain program SELEN (Spada and Stocchi, 2007), which solves the "Sea Level Equation" (SLE) in the original form of Farrell and Clark (1976) through the "pseudo-spectral" approach introduced by Mitrovica and Peltier (1991). SELEN assumes a radially stratified, incompressible Earth and a linear Maxwell viscoelastic rheology. Horizontal migration of shorelines and effects from Earth rotation instabilities are not modeled here.

The SLE reads

$$S=\frac{\rho_{\mathrm{i}}}{\gamma}G_s \otimes_i I+\frac{\rho_{\mathrm{w}}}{\gamma}G_s \otimes_o S+S^E-\frac{\rho_i}{\gamma}\overline{G_s \otimes_i I}-\frac{\rho_w}{\gamma}\overline{G_s \otimes_o S}, \qquad (1)$$

where I is the ice sheets thickness variation, ρ_i and ρ_w are densities of ice and water, respectively, $\otimes_i$ and $\otimes_o$ are spatiotemporal convolutions over the ice- and ocean-covered regions, γ is the average gravity at the Earth's surface, and the last two ocean-averaged terms ensure mass conservation. Green's sea level function G_s accounts for mantle viscoelasticity through the load-deformation coefficients for vertical displacement and incremental potential (Farrell and Clark, 1976; Spada and Stocchi, 2006, 2007). The "eustatic term" S^E represents the spatially uniform sea-level change for a rigid, non-gravitating Earth. The integral nature of the SLE [Eq. (1)] demands the recursive procedure outlined in detail by Spada and Stocchi (2007). In this study, the maximum harmonic degree is l_{max} = 96 and the spatial resolution of the icosahedron-based integration grid is R = 28 [this corresponds to a spatial discretization of 30252 pixels on the surface

of the sphere, see Tegmark (1996)].

Once S is obtained from Eq. (1), the vertical displacement and change of geoid elevation are given by

$$U = \rho_i G_u \otimes_i I + \rho_w G_u \otimes_o S, \tag{2}$$

and

$$N = \rho_i G_n \otimes_i I + \rho_w G_n \otimes_o S, \tag{3}$$

where G_u and G_n are appropriate Green functions. Variables S, U, and N obey the fundamental equation

$$S=N-U, \tag{4}$$

which defines sea-level change [see e. g. Spada and Stocchi (2006)].

By adopting the ice chronology ICE5G (Peltier, 2004), we will solve the SLE for an Earth model characterized by a 65-km thick purely elastic lithosphere with PREM-averaged density and shear modulus, and upper- and lower-mantle viscosities (henceafter η_{UM} and η_{LM}) of 3×10^{20} and 1×10^{22} Pa·s, respectively. This viscosity profile (which will be referred to as RVKL) and lithospheric thickness have been constrained by relative Holocene sea level indicators in Italy (Lambeck *et al.*, 2004a; Lambeck and Purcell, 2005; Antonioli *et al.*, 2008). To assess how GIA affects sea-level variations and vertical movements across the Italian region more robustly, we will also consider three rheological models with an increasing contrast between upper and lower mantle viscosities in the following. RVM1 is characterized by a nearly-uniform viscosity profile the with $\eta_{UM} = 10^{21}$ Pa·s and $\eta_{LM} = 2\times10^{21}$ Pa·s (Tushingham and Peltier, 1991), while in RVM2 viscosity increases by one order of magnitude ($\eta_{UM} = 4\times10^{20}$ Pa·s and $\eta_{LM} = 4\times10^{21}$ Pa·s). For RVM3, $\eta_{UM} = 4\times10^{20}$ and $\eta_{LM} = 4\times10^{22}$ Pa·s. In this study we do not consider the effects of varying the thickness of the lithosphere since, from test computations (not shown here), we have verified that this parameter generally plays a minor role compared to mantle viscosity. The role of lateral variations of lithospheric thickness in the region of interest cannot be fully addressed because of the relatively low spatial resolution of current 3D GIA models (Spada *et al.*, 2006).

3. Results

In Figs. 1, 2, and 3, we show expected values of $\dot{S}$, $\dot{U}$, and $\dot{N}$ at the present time (the dot denotes a time-derivative), which obey the fundamental relationship given by Eq. (4). In the bulk of the central Mediterranean, subsidence of the solid surface and of the geoid mainly results from the delayed effect of melt-water loading after the end of melting of the late-Pleistocene ice sheets, which according to model ICE5G occurred 4000 years ago. Rates of subsidence increase

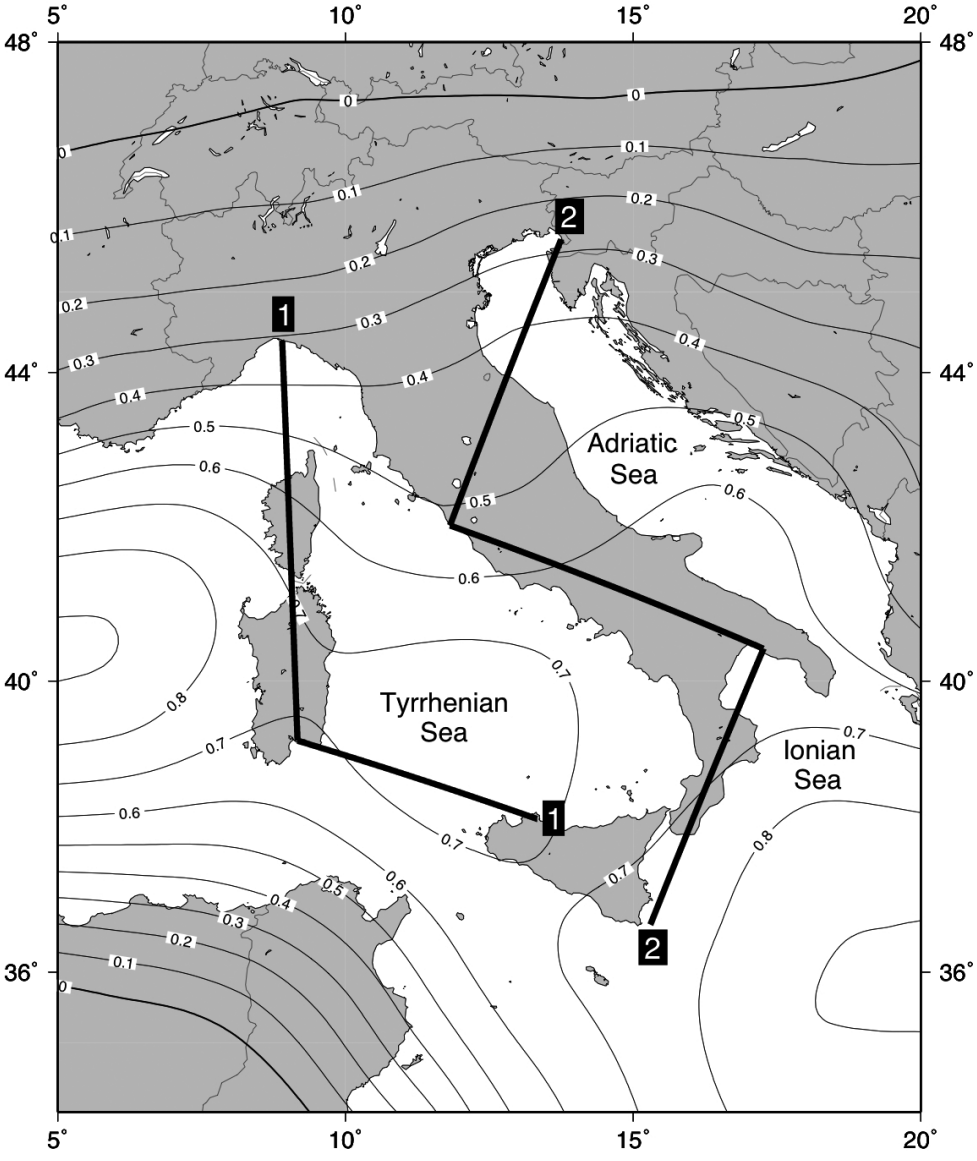

Fig. 1 - Predicted rate of present-day sea-level change $\dot{S}$ (mm yr^{-1}) according to our reference model ICE5G(RVKL). Solid lines show transects "1" and "2" considered in Fig. 7.

southward and $\dot{S}$ reaches maximum values between ~ 0.7 and 0.9 mm yr^{-1} in the bulk of the Tyrrhenian Sea (Sardinia), and between Sicily and Greece (Ionian Sea). The GIA-induced rate of sea level change shown in Fig. 1 represents a significant fraction of the average rate of sea level rise deduced by the global network of tide-gauges during the last century (in the range of 1-2 mm yr^{-1}), mainly associated with the ongoing climatic variations (Douglas, 1991; Cazenave and Nerem, 2004).

The basic data considered in this study are shown in Figs. 4, 5, and 6. The first illustrates sea

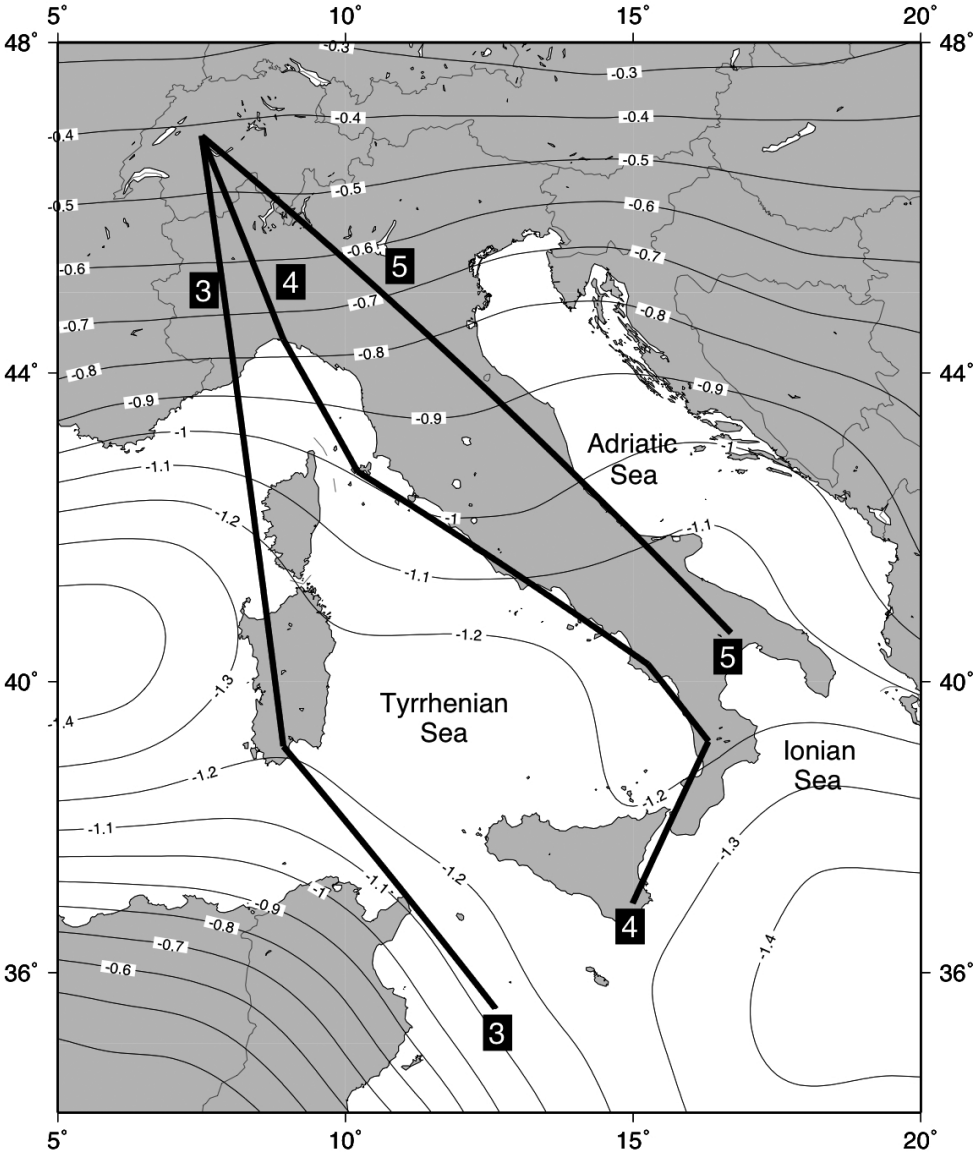

Fig. 2 - Present-day vertical velocity $\dot{U}$(mm y^{-1}), according to the same model of Fig. 1. Solid lines show transects "3", "4", and "5" discussed in the text and considered in Fig. 8.

level trends at the Italian PSMSL tide gauges network (data available from http://www.pol.ac.uk/). The French site of Marseille (Ma) and the Croatian tide gauge of Dubrovnik (Du) are also considered. Whilst Marseille records the longest time series in the Mediterranean, spanning from 1886 to 2004 with a trend of +1.2 ± 0.1 mm yr^{-1}, two other long records of Genova (Ge) and Trieste (Tr) get very close to that, Dubrovnik is of particular interest since it is representative of the southern Adriatic and it is placed close to a continuous GPS station. Fig. 5 displays all the PSMSL observations (a) and those considered in Fig. 4 (b) as

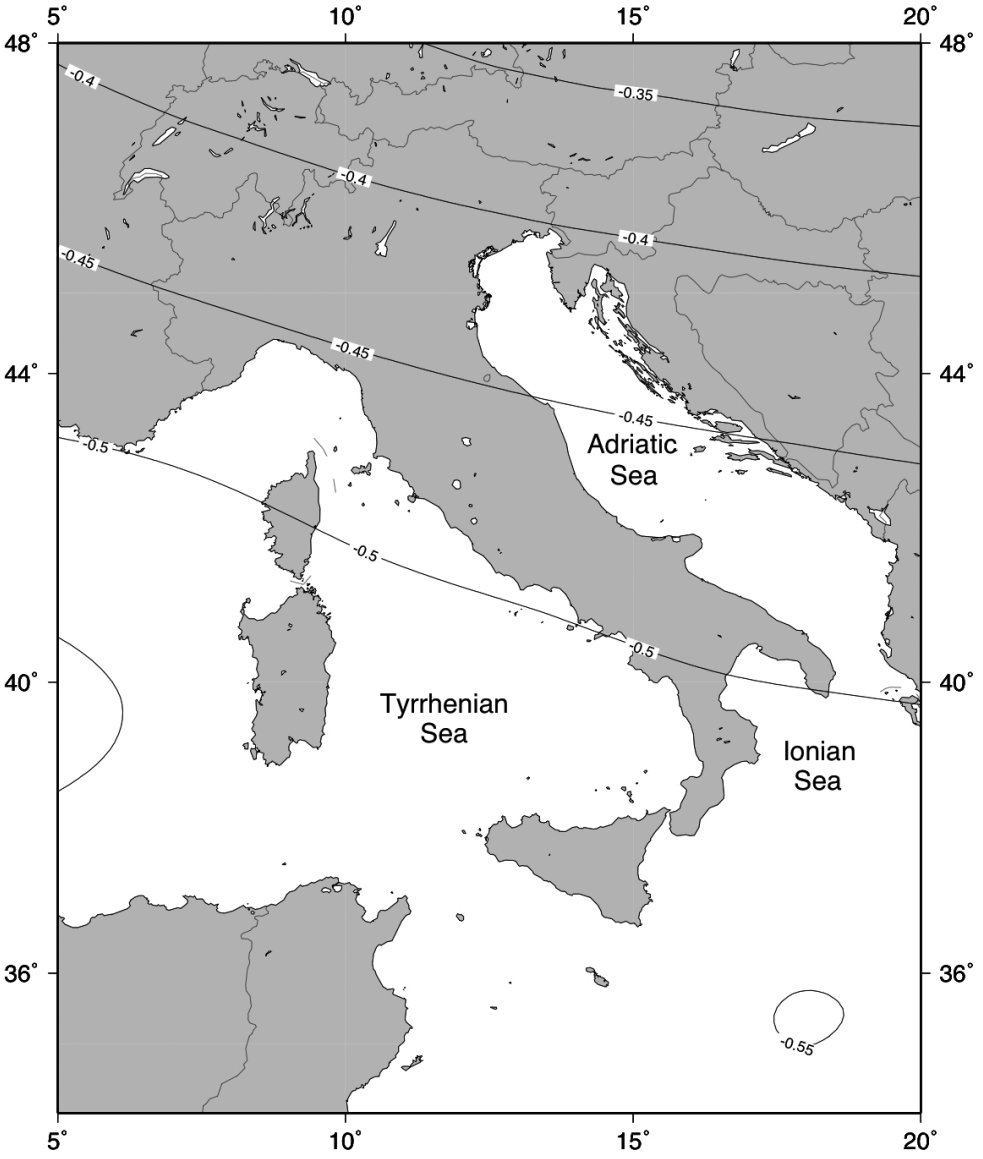

Fig. 3 - Present-day rate of change of geoid height $\dot{N}$ (mm yr^{-1}), according to the same model of Fig. 1. $\dot{N}$ is given by $\dot{S}+\dot{U}$ [see Eq. (4)], where $\dot{S}$ and $\dot{U}$ are shown in Figs. 1 and 2, respectively.

function of record length. For time-series that are shorter or equal to ~15 years, absolute values of observed rates largely exceed those expected from the longest records and show a significant scatter. According to Douglas (1992), tide gauges time series, shorter than 50 years, cannot be considered reliable indicators of sea-level rise or acceleration. The rates shown in Fig. 4 are broadly consistent with those inferred by coastal archaeological observations (Lambeck *et al.*, 2004b; Antonioli *et al.*, 2007). The latter provide relative sea-level rates from historical times (~2000 - 2400 years BP) of 0.8 mm yr^{-1} for the Sardinia, 1.1 mm yr^{-1} for northern Adriatic (but

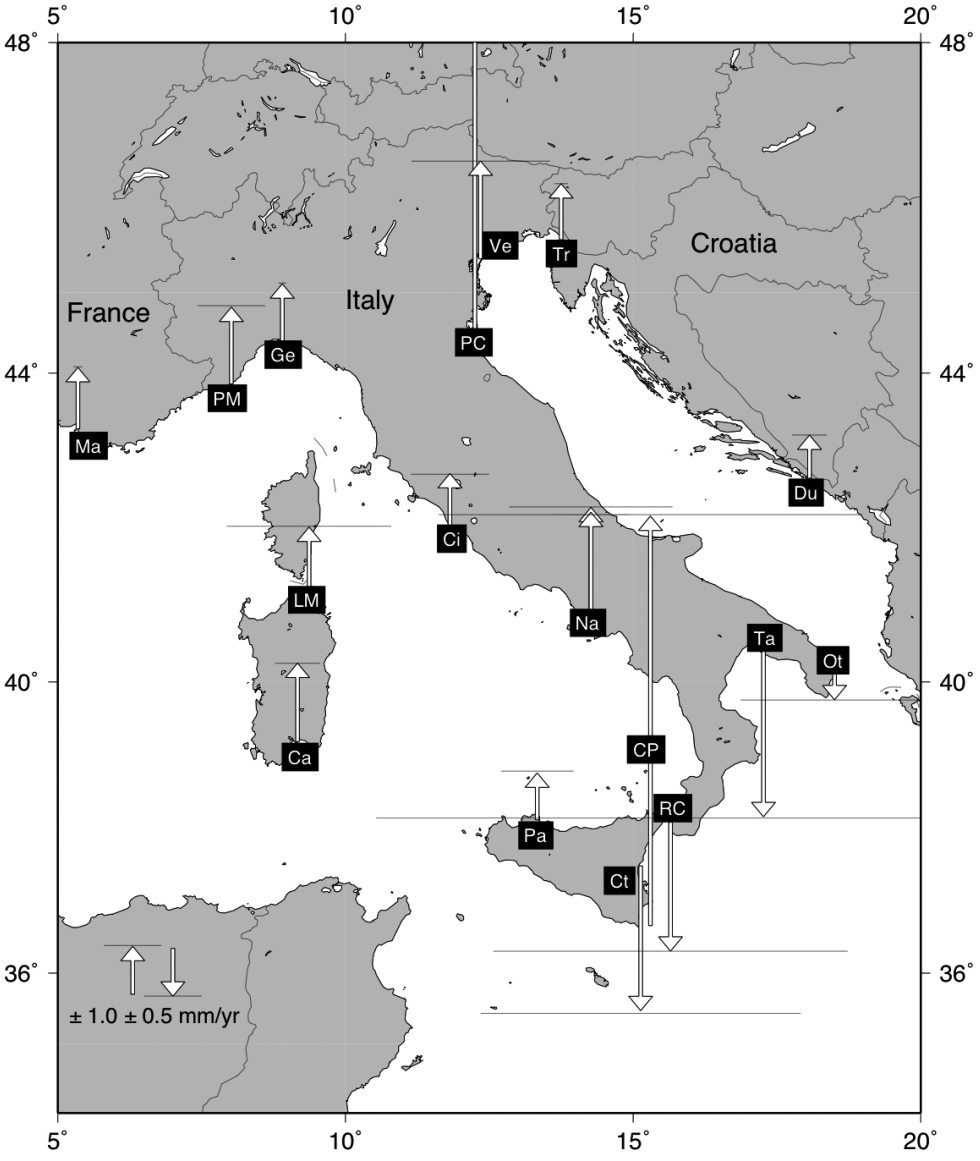

Fig. 4 - Measured rates of sea-level change at tide gauges pertaining to the PSMSL tide gauges network (a). Abbreviations refer to the Italian stations contained in the PSMSL table of mean sea-level trends (see page http://www.pol.ac.uk/psmsl/datainfo/rlr.trends), with the addition of Marseille (Ma) and Dubrovnik (Du).

for this area with an important tectonic contribution of 0.8 mm yr^{-1}) and 0.7 mm yr^{-1} for the peninsular coast of the Tyrrhenian Sea. Rates of GPS vertical velocity, considered in Fig. 6, represent residual, vertical velocities computed by means of a distributed processing approach and refer to the stable Corsica-Sardinia block, and are consistent with Table 4 and Fig. 6b of Serpelloni *et al.* (2006).

To compare the numerical results with the observed rates of Figs. 4 and 6, we now compute $\dot{S}$

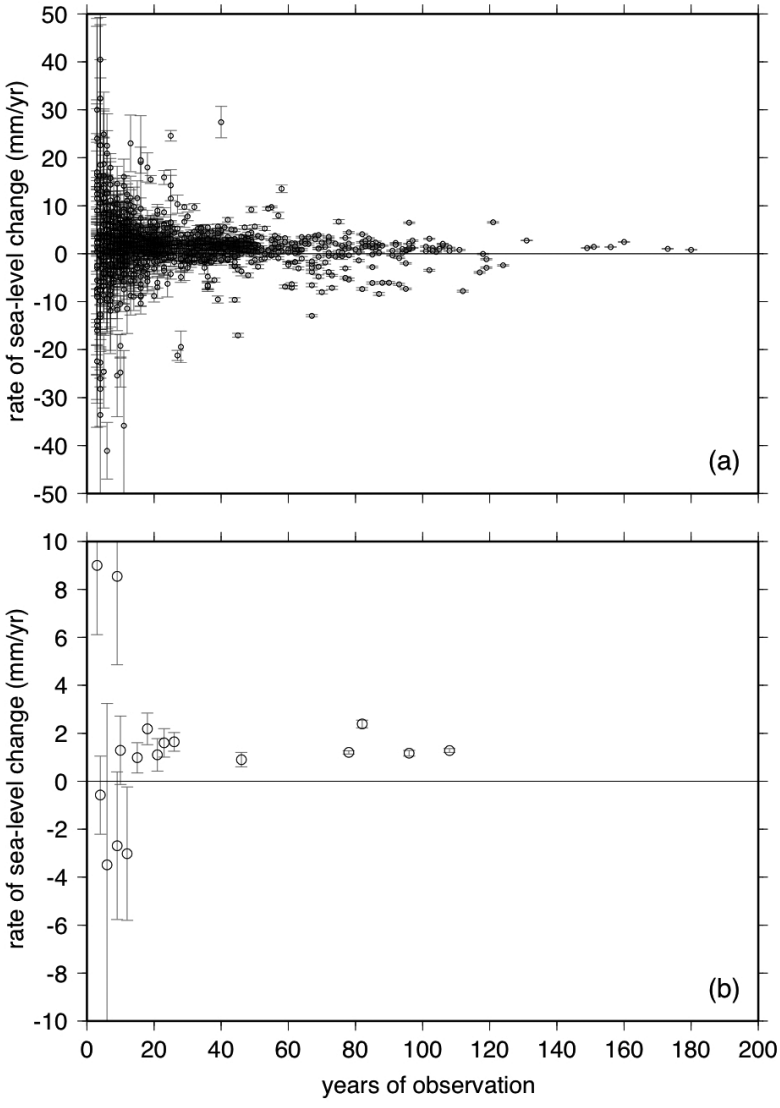

Fig. 5 - Rate of sea-level change according to PSMSL as a function of the period of observation for all tide gages (a), and those considered in this study (b).

and $\dot{U}$ using ICE5G and the viscosity profiles RVM1, RVM2, RVM3 and RVKL. Fig. 7a shows, as a function of latitude, observed $\dot{S}$ values and predictions along transect "1" of Fig. 1, connecting Genova (Ge) to Palermo (Pa), and crossing Sardinia (LM, Ca) (numbers in parentheses indicate the period of observation for each station). Though the 96-year-long time-series of Genova is possibly the only one suitable for a reliable estimate of secular trend (Zerbini *et al.*, 1996), the other Tyrrhenian tide gauges clearly indicate, from the end of nineteenth to the first decades of the twentieth century, positive rates that vary between 1.0 and 1.6 mm yr^{-1},

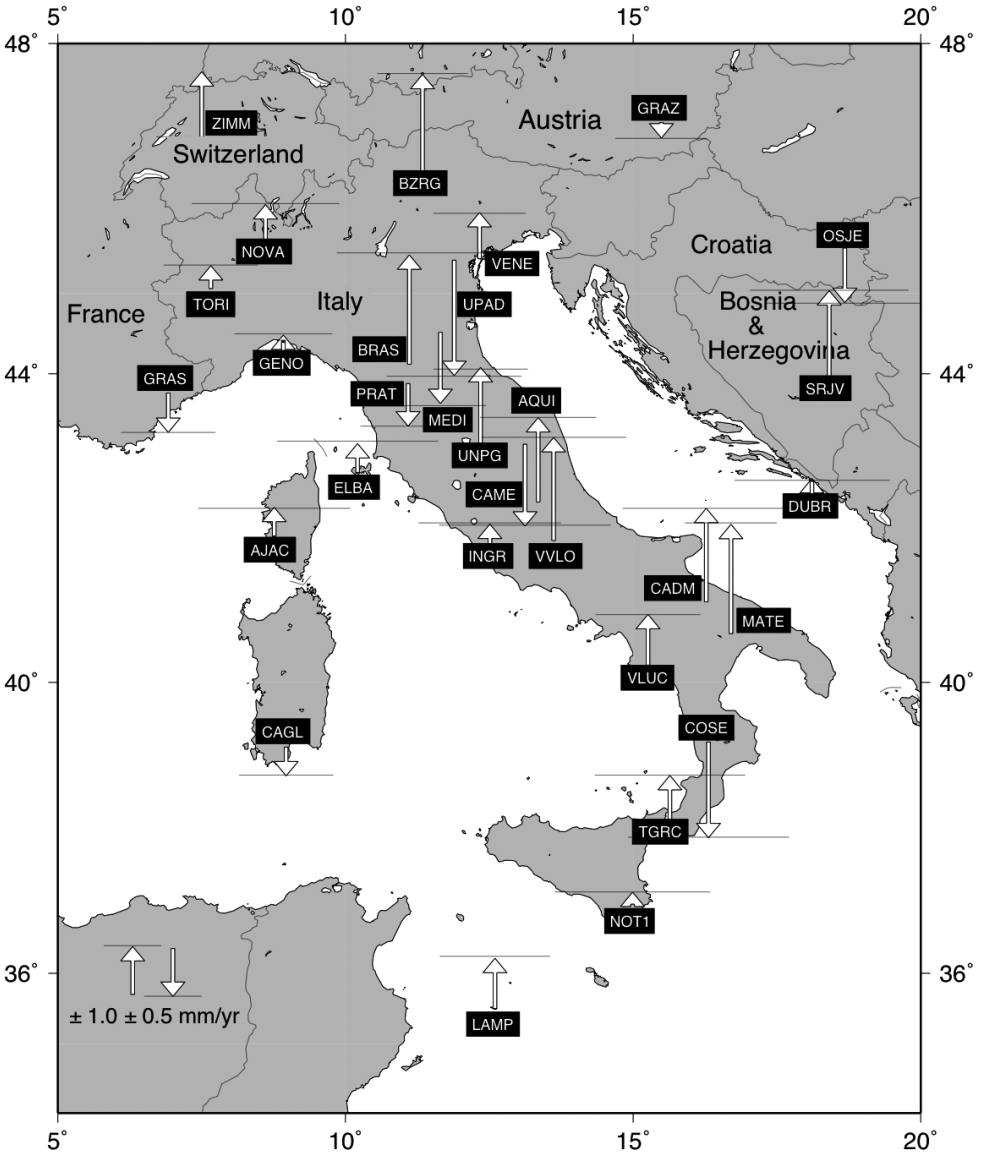

Fig. 6 - Vertical velocity solutions referred to the stable Corsica-Sardinia block from continuous GPS stations of Table 4 in Serpelloni *et al*. (2006).

consistent with Ge. The observed sea-level rise shows the same trend (grey spline) in the predictions, with a tendency to increase southwards. The lowest values are obtained for the RVM1 model (dotted), with a sea-level fall of -0.2 mm yr^{-1} in Genova. With increasing contrast between η_{UM} and η_{LM}, model results shift progressively towards larger values as a consequence of the increased isostatic disequilibrium. For models RVKL and RVM3, GIA explains a large fraction of observed sea level rise, and leaves a residual of climatic origin that does not exceed 1 mm yr^{-1}, below the estimated average rate during the last century (Douglas, 1991; Douglas *et al.*, 2000;

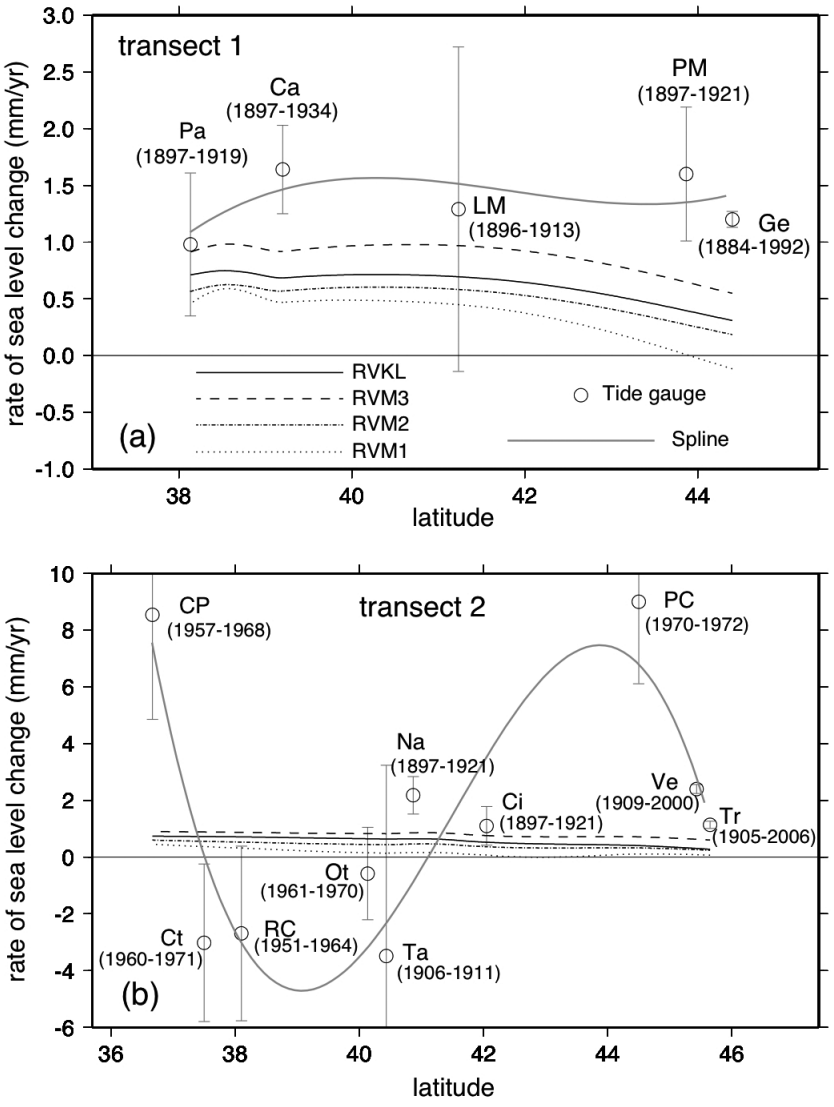

Fig. 7 - Observed (a) and computed (b) $\dot{S}$ along the two transects shown in Fig. 1, respectively. Station abbreviations are as in Fig. 4. Rates and their uncertainties are computed using the PSMSL annual 'RLR' (Revised Local Reference) data-set (see http://www.pol.ac.uk/psmsl/) by straightforward least squares. The time interval used for rate calculation is shown next to each datum. The grey curve is a cubic regression spline of observed $\dot{S}$ values.

Church *et al.*, 2001). This agrees with findings of Tsimplis *et al.* (2005) and Marcos and Tsimplis (2007).

Model calculations and observations along transect "2" of Fig. 1, which connects the northeastern Adriatic (Tr, Ve) to the Ionian sea (Ct) hitting the central the Tyrrhenian coast and crossing the central and southern Apennines, are shown in Fig. 7b. Tide gauges in Napoli (Na) and Venezia (Ve), which are significantly affected by local geological and anthropogenic factors [e.g. Carminati and Di Donato (1999)] record rates in excess of 2 mm yr^{-1}. Disagreement between

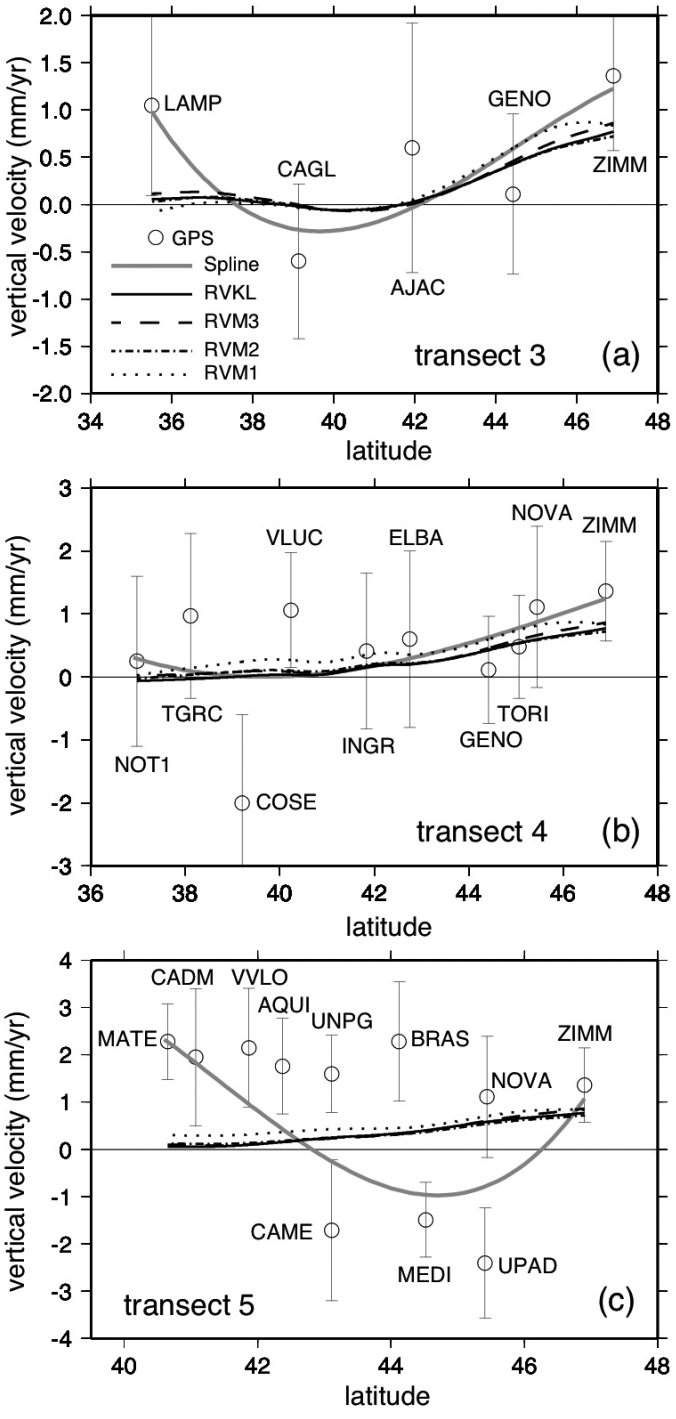

Fig. 8 - Observed and modeled $\dot{U}$ at GPS stations placed along the three transects in Fig. 2. The grey curve is a cubic regression spline of observed $\dot{U}$ values.

predictions and observations from the remaining southern tide gauge stations, which record a sea-level fall, may be attributed to local tectonic effects (Ferranti *et al.*, 2006) and to the short duration of sea-level records (see also Fig. 5).

In Fig. 8, the GPS vertical velocities of Fig. 6 are compared with predictions along the three transects shown in Fig. 2. Observed vertical velocities are residuals computed by removing the average value of CAGL and AJAC (Serpelloni *et al.*, 2006) from each solution. The same correction is applied to the expected $\dot{U}$ values. In Fig. 8a, we consider transect "3", connecting the Swiss station of ZIMM to the central Mediterranean (LAMP). Model calculations define a narrow band whose trend agrees with the cubic regression of data displayed by the grey spline. A satisfactory agreement is also obtained for transect "4" running along the Tyrrenhian coast of Italy, from ZIMM to NOT1, as shown in Fig. 8b. Both Figs. 8a and 8b clearly show that the long-wavelength pattern of vertical displacement, transects "3" and "4", is essentially driven by GIA. When the NW-SE trending path "5" of Fig. 2 is considered (see Fig. 8c), the agreement with GIA predictions is disrupted to indicate that present-day vertical velocities along the Apennines mainly

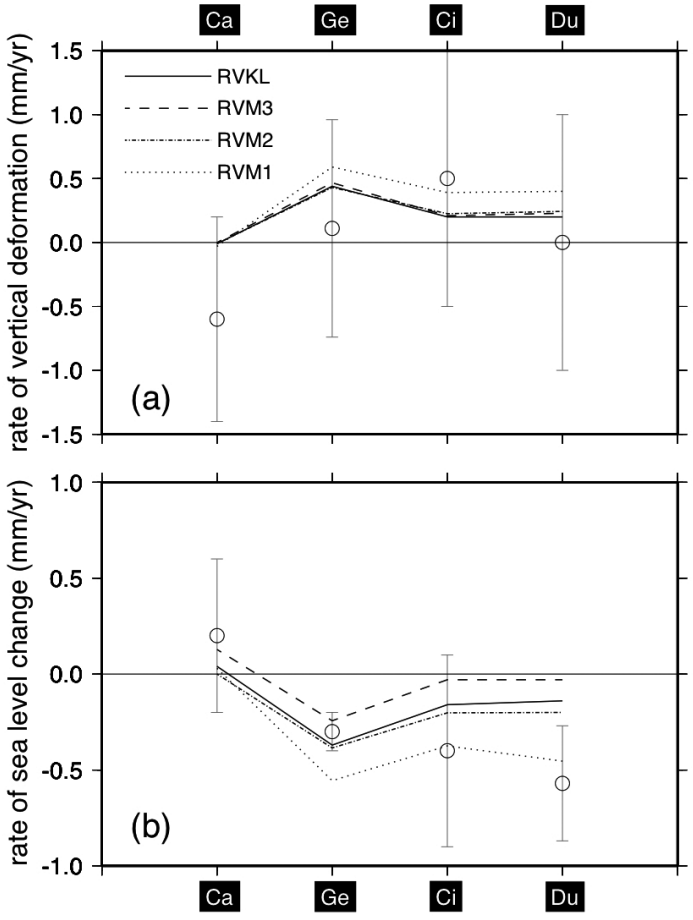

Fig. 9 - Predicted $\dot{U}$ (a) and $\dot{S}$ (b) at the sites of Cagliari (Ca), Genova (Ge), Civitavecchia (Ci), and Dubrovnik (Du), compared to GPS (a) and tide-gauge observations (b) for model RVKL and the other three mantle viscosity profiles discussed in the text.

result from local factors of geological and tectonic origin. Calculated and measured velocities clearly show opposite trends with varying latitude.

To better describe to what extent the spatial variability of current sea level change and vertical movements in Italy is driven by GIA, we consider $\dot{S}$ and $\dot{U}$ at the coastal sites of Cagliari, Genova, Civitavecchia and Dubrovnik (see Fig. 4) in Fig. 9, where both tide gauges and GPS observations are available (for Civitavecchia, we consider the average vertical velocity of nearby stations INGR and ELBA in Fig. 6). Since observed and modeled vertical velocities are referred to the Corsica-Sardinia block (as described above), sea-level trends refer to the average value of Cagliari and La Maddalena. Since $\dot{N}$ shows little variability across the study region (see Fig. 3), if GIA were the major driving process from Eq. (4), we would expect an anticorrelation between $\dot{S}$ and $\dot{U}$, and an agreement between predictions and observations. From the results of Fig. 9, the spatial variability of the referenced instrumental vertical velocities is in fact consistent with the GIA signal for all the viscosity profiles adopted, which define a narrow band within the error

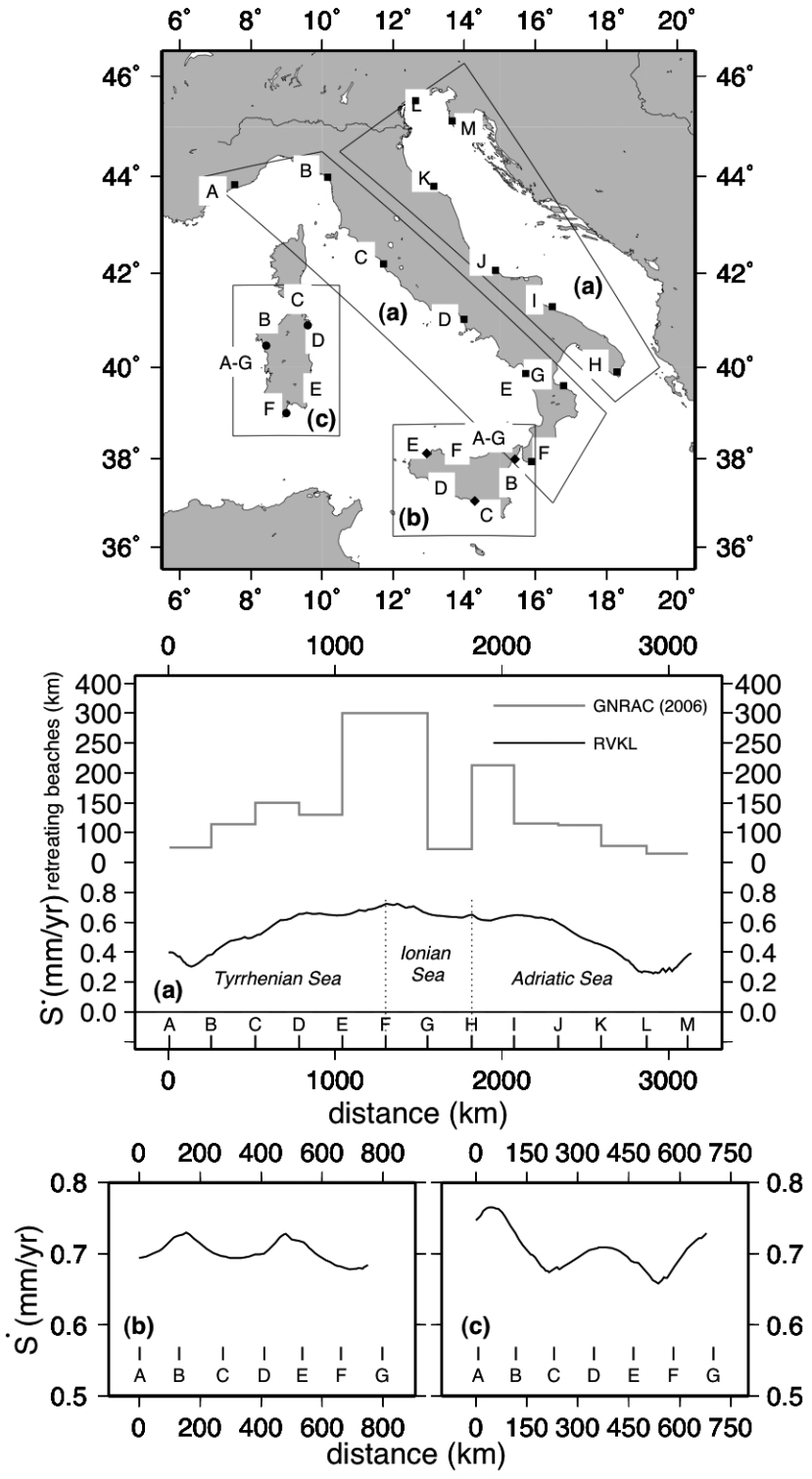

Fig. 10 - Predicted $\dot{S}$ for ICE5G(RVKL) and estimated length of retreating beaches according to GNRAC (2006), relative to the Italian peninsula (a), Sicily (b), and Sardinia (c).

observation, the tide gauge and GPS signals considered here have been significantly affected by the GIA and show broadly consistent rates.

According to recent estimates, at least 70% of the world's beaches are experiencing a permanent retreat in response to extreme phenomena (e.g. storm waves) exacerbated by global sea-level rise (Day, 2004). It is known that quantifying the relationship between sea level rise and beach erosion is not straightforward and that no universally accepted model of shoreline retreat has yet been developed (Cooper and Pilkey, 2004). The sensitivity of erosion to the sea-level rise has been (and can be) tentatively studied using the Bruun rule (e.g. Bruun, 1988), which predicts that the beach profile will shift landwards by an amount $s/\tan\vartheta$, where s is sea level rise and ϑ is the profile slope angle. Although the Bruun rule omits many important variables (Cooper and Pilkey, 2004) and fails in specific areas [see e.g. Dickson *et al.* (2007)], the sea-level rise is recognized as one of the most important factors contributing to beach erosion, mainly operating by the increased destructive power of storms (Day, 2004).

Since the GIA determines a long-wavelength, non-uniform secular sea-level rise that may reach an amplitude close to 1 mm yr^{-1} (see Fig. 1), we wonder whether it may indirectly influence current rates of erosion and beach retreat along the coastlines of Italy. To provide a tentative answer, we assume our reference model ICE5G(RVKL) and compute $\dot{S}$ along the coastlines of the Italian peninsula (see Fig. 10a), Sicily (Fig. 10b) and Sardinia (Fig. 10c). Fig. 10a shows that rates of sea-level variation always exceed 0.3 mm yr^{-1} and increase southwards where rates of ~0.75 mm yr^{-1} are expected in the Calabrian region (Ionian Sea). According to the extensive review of GNRAC (2006), a similar trend is observed for the estimates of coastal erosion, which in Fig. 10a is expressed in terms of length of retreating beaches (km) for an equal-length of coastal traits (grey stepwise curve) based on the regional study shown in the GNRAC Table of page 6.

Though estimates of regional coastal retreat are affected by large uncertainties, due in part to positive and negative feedbacks of man-made structures and human-driven imbalance of sediment supply (GNRAC, 2006), Fig. 10a shows that the trend of the beach retreat broadly follows that of the GIA-induced rate of sea-level change, with a tendency to increase towards the south of the peninsula. Available data do not allow to discern spatial trends in Sicily and Sardinia (Figs. 10b and 10c), where 440 and 170 km of beaches are retreating, respectively, and relatively large rates of GIA-related sea-level rise are expected. The non-linear relationship between sea-level rise and beach erosion is manifest observing that while southern Calabria is presently uplifting in response to tectonic forces (Ferranti *et al.*, 2006), according to GNRAC (2006) the length of retreating beaches reaches its maximum in this region (Fig. 10c).

4. Conclusions

Our analysis provides new estimates of current sea-level variations and vertical land movements along the coasts of Italy in response to GIA, which, since the end of the last deglaciation, resulted in a generalized subsidence of the Italian peninsula. At specific sites, where tide gauges and continuous GPS stations are operating, GIA provides a significant contribution to observed rates, which vary according to assumptions regarding the viscosity contrast across the 670-km depth seismic discontinuity. According to our findings, GIA modulates the long-wavelength pattern of present-day sea-level change and vertical motions along the coasts of the

Tyrrhenian Sea, but cannot explain vertical movements determined by GPS observations across the Apennines.

Present-day GIA-induced sea-level variations are not spatially uniform along the coasts of Italy. Rather, they systematically increase towards low latitudes reaching an amplitude of ~0.8 mm yr^{-1} in the Ionian Sea and are superimposed with regard to the global signal associated with recent climatic forcing (Douglas, 1991), which may be assumed to be constant across the study region. For the first time, we have shown that at long-wavelengths this pattern is correlated with the length of retreating beaches for unit coastal traits (GNRAC, 2006), which supports the existence of a close (but complex) relationship between post-glacial sea-level rise and coastal erosion (Day, 2004).

Acknowledgments. We thank Enzo Mantovani and an anonymous reviewer for their helpful suggestions. Work funded by MIUR (Ministero dell'Istruzione, dell' Università e della Ricerca) by the PRIN2006 grant "Il ruolo del riaggiustamento isostatico post-glaciale nelle variazioni del livello marino globale e mediterraneo: nuovi vincoli geofisici, geologici, ed archeologici". The numerical code employed in this study (SELEN, see http://flocolleoni.free.fr/SELEN.html) is freely available and can be requested from Giorgio Spada (email: giorgio.spada@gmail.com).

REFERENCES

Antonioli F., Anzidei M., Lambeck K., Auriemma R., Gaddi D., Furlani S., Orrù P., Solinas E., Gaspari A., Karinja S., Kovaciè V. and Surace L.; 2007: *Sea-level change during the Holocene in Sardinia and in the northeastern Adriatic (central Mediterranean Sea) from archaeological and geomorphological data*. Quat. Sci. Rev., **26**, 2463-2486.

Antonioli F., Ferranti L., Fontana A., Amorosi A.M., Bondesan A., Braitenberg C., Dutton A., Fontolan G., Furlani S., Lambeck K., Mastronuzzi G., Monaco C., Spada G. and Stocchi P.; 2009: *Holocene relative sea-level changes and vertical movements along the Italian and Istrian coastlines.* Quat. Int., in press.

Bruun P.; 1988: *The Bruun rule of erosion by sea level rise: a discussion of large-scale two- and three-dimensional usages*. J. Coast. Res., **4**, 627-648.

Carminati E. and Di Donato G.; 1999: *Separating natural and anthropogenic vartical movements in fast subsiding areas: the Po plain (N. Italy) case.* Geophys. Res. Lett., **26**, 2291-2294.

Cazenave A. and Nerem R.S.; 2004: *Present-Day sea level change: observations and causes.* Rev. Geophys., **42**, RG3001, doi: 10.1029/2003RG000139.

Church J.A., Gregory J.M., Huybrechts P., Kuhn M., Lambeck K., Nhuan M.T., Qin D. and Woodworth P.L.; 2001: *Changes in sea level.* In: Houghton J.T. *et al*. (eds), Climate Change 2001: The Scientific Basis: Contribution of Working Group I to the Third Assessment Report of the Intergovernmental Panel on Climate Change, Cambridge Univ. Press, New York, pp. 639-694.

Clark J.A. and Lingle C.S.; 1979: *Predicted relative sea-level changes (18.000 Years B.P. to present) caused by late glacial retreat of Antarctic Ice Sheet.* Quat. Res., **11**, 279-298.

Cooper J.A.G. and Pilkey O.H.; 2004: *Sea-level rise and shoreline retreat: time to abandon the Bruun rule.* Global Planet. Change, **43**, 157-171.

Day C.; 2004: *Sea-level rise exacerbates coastal erosion.* Phys. Today, <http://www.physicstoday.org/vol-57/iss-2/p24.html>.

Dickson M.E., Walkden M.J.A. and Hall J.W.; 2007: *Systemic impacts of climate change on an eroding coastal region over the twenty-first century.* Clim. Change, **84**, 141-166.

Douglas B.C.; 1991: *Global sea level rise.* J. Geophys. Res., **96,** 6981-6992.

Douglas B.C.; 1992: *Global sea level acceleration.* J. Geophys. Res., **97**, 12699-12706.

Douglas B.C., Kearney M.S. and Leatherman S.P.; 2000: *Sea Level Rise: History and Consequences.* Academic Press,

232 pp.

Farrell W.E. and Clark J.A.; 1976: *On postglacial sea level.* Geophys. Jour. R. Astron. Soc., **46**, 647-667.

Ferranti L., Antonioli F., Mauz B., Amorosi A., Dai Pra G., Mastronuzzi G., Monaco C., Orrù P., Pappalardo M., Radtke U., Renda P., Romano P., Sansò P. and Verrubbi V.; 2006: *Markers of the last interglacial sea-level high stand along the coast of Italy: Tectonic implications.* Quat. Int., **145-146**, 30-54.

GNRAC (Gruppo Nazionale per la Ricerca sull'Ambiente Costiero); 2006: *Studi Costieri*, **10**, 174 pp.

Lambeck K. and Johnston P.; 1995: *Land subsidence and sealevel change: contributions from the melting of the last great ice sheets and the isostatic adjustment of the Earth.* In: Barends F.B.J. *et al*. (eds), Land Subsidence. Balkema, Rotterdam, pp. 3-18.

Lambeck K. and Purcell A.; 2005: *Sea-level change in the Mediterranean Sea since th LGM: model predictions for tectonically stable areas.* Quat. Sci. Rev., **24**, 1969-1988.

Lambeck K., Antonioli F., Purcell A. and Silenzi S.; 2004a: *Sea level change along the Italian coast from the past 10,000 yr.* Quat. Sci. Rev., **23**, 1567-1598.

Lambeck K., Anzidei M., Antonioli F., Benini A. and Esposito A.; 2004b: *Sea level in Roman time in the Central Mediterranean and implications for recent change.* Earth Planet. Sci. Lett., **224**, 563-575.

Marcos M. and Tsimplis M.N.; 2007: *Forcing of coastal sea level rise patterns in the North Atlantic and the Mediterranean Sea.* Geophys. Res. Lett., **34**, doi:10.1029/2007GL030641.

Mitrovica J.X. and Peltier W.R.; 1991: *On post-glacial geoid subsidence over the equatorial ocean.* J. Geophys. Res., 96, 20,053-20,071.

Peltier W.R.; 2004: *Global glacial isostasy and the surface of the Ice-Age Earth: the ICE-5G(VM2) model and GRACE.* Annu. Rev. Earth Pl. Sc., **32**, 111-149.

Pirazzoli P.A.; 1991: *World atlas of Holocene sea-level changes.* Elsevier, Amsterdam, 300 pp.

Pirazzoli P.A.; 2005: *A review of possible eustatic, isostatic, and tectonic contributions in eight late-Holocene relative sea-level histories from the Mediterranean area.* Quat. Sci. Rev., **24**, 1989-2001.

Serpelloni E., Casula G., Galvani A., Anzidei M. and Baldi P.; 2006: *Data analysis of permanent GPS networks in Italy and surrounding regions: Application of a distributed processing approach.* Ann. Geophys., **49**, 897-928.

Spada G. and Stocchi P.; 2006: *The Sea Level Equation, Theory and Numerical Examples.* Aracne, Roma, 96 pp.

Spada G. and Stocchi P.; 2007: *SELEN: a Fortran 90 program for solving the "Sea Level Equation".* Comput. Geosci., **33**, doi: 10.1016/j.cageo.2006.08.006.

Spada G., Antonioli A., Cianetti S. and Giunchi C.; 2006: *Glacial isostatic adjustment and relative sea-level changes: the role of lithospheric and upper mantle heterogeneities in a 3-D spherical Earth.* Geophys. J. Int., **165**, doi: 10.1111/j.1365- 246X.2006.02969.x

Stocchi P. and Spada G.; 2007: *Glacio and hydro-isostasy in the Mediterranean Sea: Clark's zones and role of remote ice sheets.* Ann. Geophys., **50** (6), 741-761.

Stocchi P., Spada G. and Cianetti S.; 2005: *Isostatic rebound following the Alpine deglaciation: impact on the sealevel variations and vertical movements in the Mediterranean region.* Geophys. J. Int., **162**, doi: 10.1111/j.1365-246X.2005.02653.x.

Tegmark M.; 1996: *An icosahedron-based method for pixelizing the celestialsphere.* ApJ Letters, **470**, L81-L84.

Tsimplis M.N., Alvarez-Fanjul E., Gomis D., Fenoglio-Marc L. and Pérez B.; 2005: *Mediterranean Sea level trends: Atmospheric pressure and wind contribution.* Geophys. Res Lett., **32**, doi:10.1029/2005GL023867.

Tushingham A.M. and Peltier W.R.; 1991: *Ice-3G: a new global model of late Pleistocene deglaciation based upon geophysical prediction of post-glacial sea level change*. J. Geophys. Res., **96**, 4497-4523.

Zerbini S., Plag H.P., Baker T., Becker M., Billiris H., Burki B., Kahle H.G., Marson I., Pezzoli L., Richter B., Romagnoli C., Sztobryn M., Tomasi P., Tsimplis M., Veis G. and Verrone G.; 1996: *Sea level in the Mediterranean: a first step towards separating crustal movements and absolute sea-level variations*. Global Planet. Change, **14**, 1-48.

Corresponding author: Giorgio Spada
Istituto Fisica
Università di Urbino "Carlo Bo"
Via Santa Chiara 27, 61029 Urbino (Italy)
phone: +39 0722 303389; fax: +39 0722 303399; e-mail: giorgio.spada@gmail.com